Iranian Journal of Medical Physics
Vol. 8, No. 1, Winter 2012, 65-74
Received: January 19, 2012; Accepted: February 01, 2012

Original Article

A Comparison of the Dosimetric Parameters of Cs-137 Brachytherapy Source in Different Tissues with Water Using Monte Carlo Simulation

Sedigheh Sina[1], Reza Faghihi[1,2*], Ali Soleymani Meigooni[3]

Abstract

Introduction
After the publication of Task Group number 43 dose calculation formalism by the American Association of Physicists in Medicine (AAPM), this method has been known as the most common dose calculation method in brachytherapy treatment planning. In this formalism, the water phantom is introduced as the reference dosimetry phantom, while the attenuation coefficient of the sources in the water phantom is different from that of different tissues. The purpose of this study is to investigate the effects of the phantom materials on the TG-43 dosimetery parameters of the Cs-137 brachytherapy source using MCNP4C Monte Carlo code.
Materials and Methods
In this research, the Cs-137 (Model Selectron) brachytherapy source was simulated in different phantoms (bone, soft tissue, muscle, fat, and the inhomogeneous phantoms of water/bone) of volume 27000 cm3 using MCNP4C Monte Carlo code. *F8 tally was used to obtain the dose in a fine cubical lattice. Then the TG-43 dosimetry parameters of the brachytherapy source were obtained in water phantom and compared with those of different phantoms.
Results
The percentage difference between the radial dose function g(r) of bone and the g(r) of water phantom, at a distance of 10 cm from the source center is 20%, while such differences are 1.7%, 1.6% and 1.1% for soft tissue, muscle, and fat, respectively. The largest difference of the dose rate constant of phantoms with those of water is 4.52% for the bone phantom, while the differences for soft tissue, muscle, and fat are 1.18%, 1.27%, and 0.18%, respectively. The 2D anisotropy function of the Cs-137 source for different tissues is identical to that of water.
Conclusion
The results of the simulations have shown that dose calculation in water phantom would introduce errors in the dose calculation around brachytherapy sources. Therefore, it is suggested that the correction factors of different tissues be applied after dose calculation in water phantoms, in order to decrease the errors of brachytherapy treatment planning.

Keywords: Brachytherapy, MCNP4, Monte Carlo

1- School of Mechanical Engineering, Nuclear Engineering Department, Shiraz University, Shiraz, Iran
*Corresponding author: Tel: +987116473474; email: faghihir@shirazu.ac.ir
2- Radiation Research Center, Shiraz University, Shiraz, Iran
3- Comprehensive Cancer Center of Nevada, 3730 S. Eastern Ave., Las Vegas, Nevada, USA

1. Introduction

Prior to the introduction of the Task group number 43 (TG-43) dosimetry formalism, calculations of the brachytherapy dosimetry methods were based on the old methods using the apparent activity of the brachytherapy sources and the exposure rate constant (Γ). These methods require the exact determination of the attenuation coefficients of the photons in the phantoms and the effective mass attenuation coefficient of the photons in the source encapsulation [1], while determining the effective mass attenuation coefficient for the sources of complex geometries such as I-125 and Pd-103 can be quite challenging. In order to overcome such difficulties, the American Association of the Physicists in Medicine (AAPM) introduced a new dosimetry formalism in TG-43 [2]. According to the recommendations of this formalism, the dosimetric parameters of each brachytherapy source should be determined by two investigators using the Monte Carlo simulations or experimental measurements and be presented in tabular forms. As the TG-43 dosimetric parameters of brachytherapy sources are obtained by the direct measurement or simulation of the dose at different points inside the phantom, there is no need to determine the effective mass attenuation coefficient of the filters and the source encapsulation. In addition, the calculations of the TG-43 parameters are not dependent on the apparent activity and the exposure rate constant.

Although the TG-43 dose calculation formalism is known as the main dosimetric method in the Treatment Planning Systems (TPS), many investigators have investigated its main deficiencies, i.e., performing the dosimetry in homogeneous water phantom, not considering the effect of phantom size, and not taking the attenuations of photons caused by the applicators and other sources into account [3-9].

Based on the recommendations of the AAPM TG-43, the Monte Carlo simulations for determination of the dosimetry parameters should be performed in a homogeneous water phantom. As the attenuation, scattering, and absorption coefficients of the different tissues are different from those of water phantom, the dose calculation in water would be the cause of the errors in dose calculations of the TPSs. The purpose of this study is to determine the TG-43 parameters of the Cs-137 brachytherapy source in different phantoms, i.e. soft tissue, bone, fat, muscle, and the inhomogeneous phantom composed of water and bone using MCNP4C Monte Carlo code, and to compare the dosimetric parameters of each phantom with those of water.

2. Materials and Methods

2.1. TG-43 dose calculation formalism

In 1995, the American Association of Physicists in Medicine (AAPM) published the TG-43 for the dosimetry of brachytherapy sources. According to the recommendations of this task group, point r_0=1 and θ_0=90° is considered as the reference point, and the dose in point P(r,θ) is calculated using equation 1 (see Figure 1).

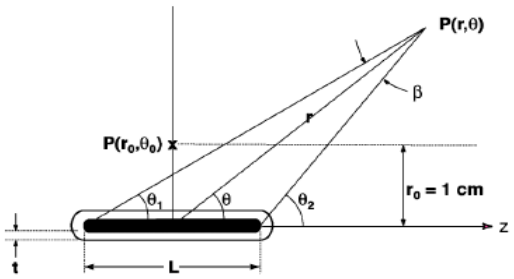

Figure 1. Coordinations used in TG-43 formalism [2]

$$\dot{D}(r,\theta) = S_k . \Lambda . \frac{G_x(r,\theta)}{G_x(r_0,\theta_0)} . g_x(r) . F(r,\theta), \qquad (1)$$

In which S_k is the air kerma strength, Λ is the dose rate constant, g(r) is the radial dose function, F(r,θ) is the anisotropy function, and G(r,θ) is the geometry function. The updates of this protocol (TG-43U1 and TG-43U1S1) were published in 2004 and 2007, respectively [2, 10].

2.2. Simulation of different phantoms

The TG-43 dosimetry parameters (i.e. dose rate constant (Λ), radial dose function ($g(r)$), and function ($F(r,\theta)$)) of the Cs-137 LDR brachytherapy source were obtained in different tissues (water, bone, four element soft tissue, muscle, and inhomogeneous phantom composed of water and bone) using MCNP4C Monte Carlo code. The density and composition of different phantoms were used according to report number 44 of the International Commission on Radiation Units and Measurements (ICRU44) [10].

The cubical phantoms for different tissues with a volume of 27000 cm^3 (30 cm×30 cm×30 cm) were simulated using MCNP4C, and the phantoms were divided into a small cubical lattice of 0.1 cm to perform the dose calculations in different points inside the phantom. The *F8 tally was used to obtain the energy deposition inside the cubical cells, and the dose rate inside each tally cell was obtained by dividing the simulation results by the mass of the tally cell, and then multiplying the result by the source activity and the number of 661.67 MeV photons per disintegration of Cs-137. The programs were run for 108 starting particles [11].

2.3. Cs-137 LDR source

The Cs-137 Low Dose Rate (LDR) Selectron brachytherapy sources are composed of spherical sources of 1.5 mm which are inside a 0.5 mm stainless steel cover. Various configurations of active sources and inactive pellets of 2.5 mm in diameter are inserted inside different applicators [8, 12-16]. For instance, a combination of 10 active pellets (AANNAANNAANNAANNAA) is one of the configurations that can be used for treatment of the patients, in which A represents active pellet and N represents non-active or dummy pellets. In this research, the dose distribution around a single source and also the dose around 10 active sources were obtained by simulation using MCNP4C. The simulated applicator in this research is the cylindrical applicator with a 0.6 cm diameter composed of several layers (0.05 cm polyethelene, 0.05 cm air, and 0.05 cm stainless steel) [15].

2.4. The effect of phantom material on dose distribution around Cs-137 source

The simulations were performed for a single source of 2.5 mm and for ten Cs-137 sources with an active length of 4.5 mm loaded in the applicator in different phantoms, i.e., soft tissue, muscle, bone, fat, and water. The dose distribution inside each phantom was then compared with the dose distribution in the water phantom. It should be mentioned that in this research, to obtain the geometry function, the $Gp(r,\theta)$ was used for the spherical source, and $GL(r,\theta)$ was used for 10 active sources, according to TG-43U1 formalism.

In a real treatment, the applicator is not placed inside or just near the bone, so the assumption of homogeneous bone phantom is not correct, thus the simulations were repeated for inhomogeneous phantom composed of layers of bone and water. The simulations were performed for three cubical phantoms of 27000 cm^3 of different configurations. The first phantom was composed of 2 cm water and 13 cm bone, the second phantom was composed of 1 cm water, and 2 cm bone, and 12 cm water, and the third was composed of 1.5 cm water, 1 cm bone, and 12.5 cm water. Figure 2 shows the simulation geometry of the first and the third phantom.

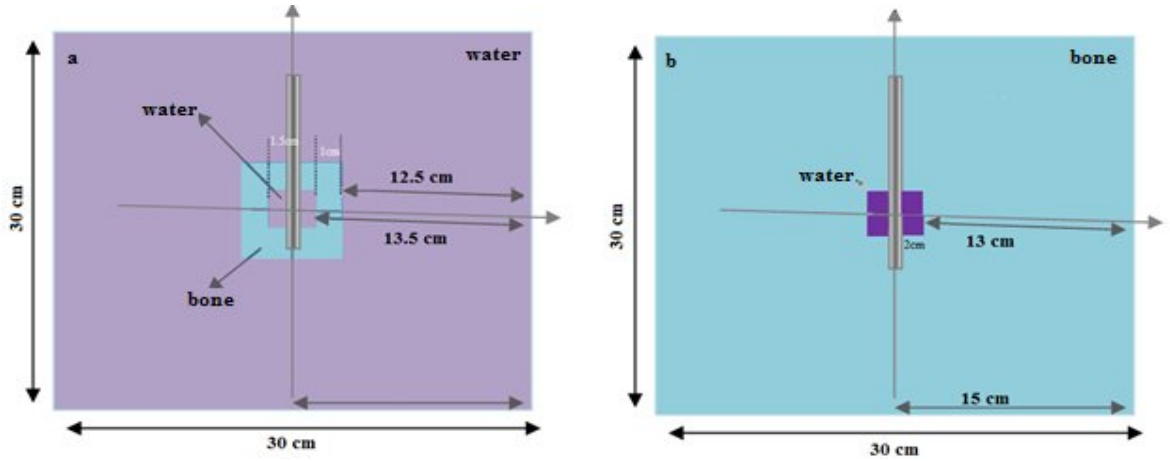

Figure 2. The geometry of simulation of inhomogeneous phantoms, a) phantom 3, and b) phantom 1

3. Results

3.1. The effect of phantom material on dose distribution around Cs-137

Comparison of the dose distribution around a spherical source inside the applicator obtained by MCNP4C in different phantoms is shown in Figure 3. The composition of the source and the applicator are obvious in this figure. Comparison of the isodose curves shows that the isodose curves for muscle, fat, and water are in close consistence with each other, while the difference between the isodose curves in bone phantom and water can be recognized clearly.

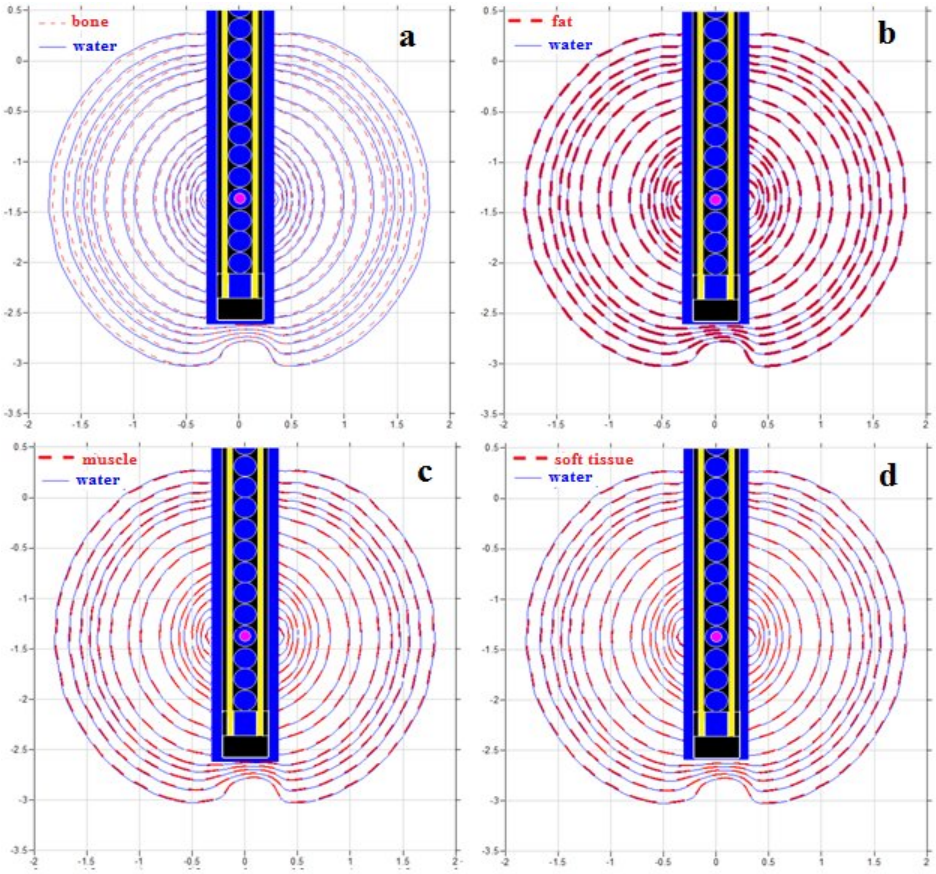

Figure 3. A comparison between the dose distributions around a single active Cs-137 pellet inside the applicator in different phantoms. a) bone-water, b) fat-water, c) muscle-water, and d) soft tissue-water.

3.2. The effect of phantom material on TG-43 parameters of Cs-137

3.2.1. The effect of phantom material on dose rate constant (Λ)

To investigate the effect of phantom material on the dose rate constant (Λ) of Cs-137, the air kerma was simulated in the air phantom and then the dose rate constant for each phantom was obtained by dividing the dose at a distance of 1 cm to the air kerma strength (SK). The dose rate constant for different phantoms and the percentage difference between this parameter at each phantom to that of water are shown in Table 1. The table also compares the results of this study with those obtained by Melhus et al. using MCNP5 [17].

As can be seen from the figure, the highest difference between the values of dose rate constant compared with water is 4.52% for the bone phantom, while such differences for soft tissue, muscle, and fat are 1.18%, 1.27%, 0.18%, respectively.

3.2.2. The effect of phantom material on radial dose function (g(r))

To simulate the effect of phantom material on the radial dose function of the Cs-137 source, a single pellet source was simulated inside the applicator in different phantoms. Figure 4 shows the ratio of g(r) in different phantoms to g(r) of water phantom.

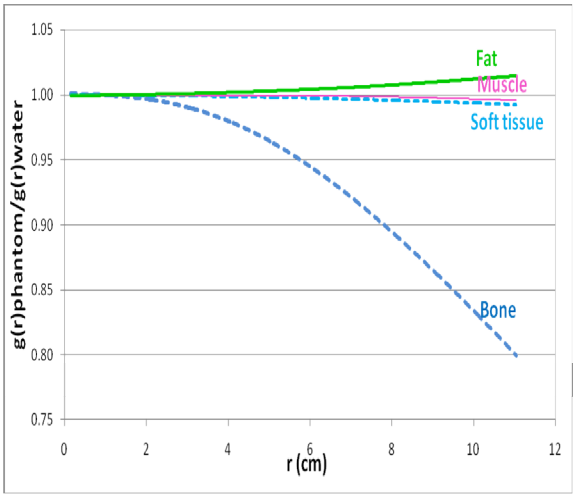

Figure 4. The ratio of the dose rate constant of different phantoms to dose rate constant of water for Cs-137 brachytherapy source.

To consider the real treatment situations, the simulations were repeated for several inhomogeneous phantoms of water and bone. The percentage difference of the dose in different phantoms with water is shown in Figure 5. As is obvious from the figure, in all inhomogeneous phantoms, the dose increases at the water-bone boundary, and decreases when entering the bone.

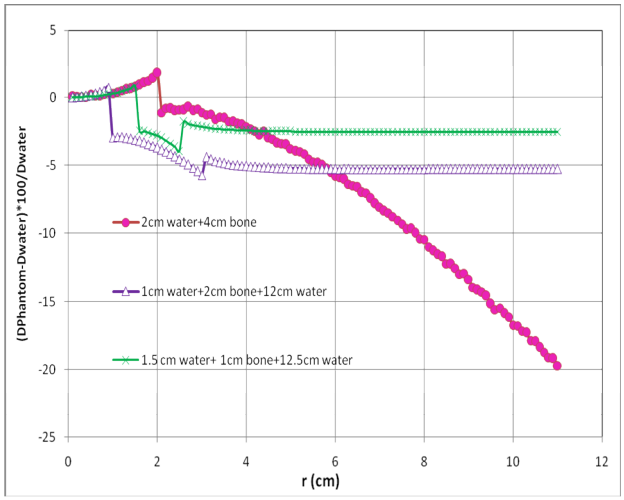

Figure 5. percentage difference between the dose in inhomogeneous phantom of water/bone) with the dose in water phantom for Cs-137 source.

3.2.3. The effect of phantom material on anisotropy function (F(r,θ))

In this section, to investigate the effect of phantom material on the anisotropy function around the Cs-137 source inside the applicator, the ratio of dose values at different distances and 45 degree angle of the phantom (D(r,45°)Phantom) to the water dose at the same points (D(r,45°)Water) was obtained. Figure 6 shows that the maximum percentage difference between the dose at an angle of 45 degrees in tissues to the dose in water is observed for bone such that this dose ratio is 0.96 for the distance of 5 cm.

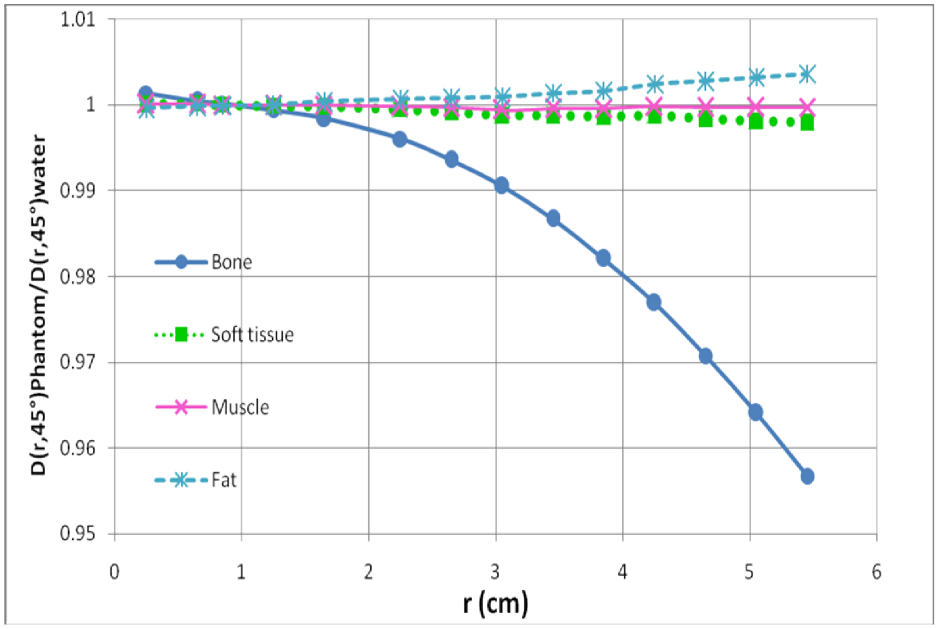

Figure 6. The ratio of dose at different distance and angle=45° in different phantoms to the dose in water.

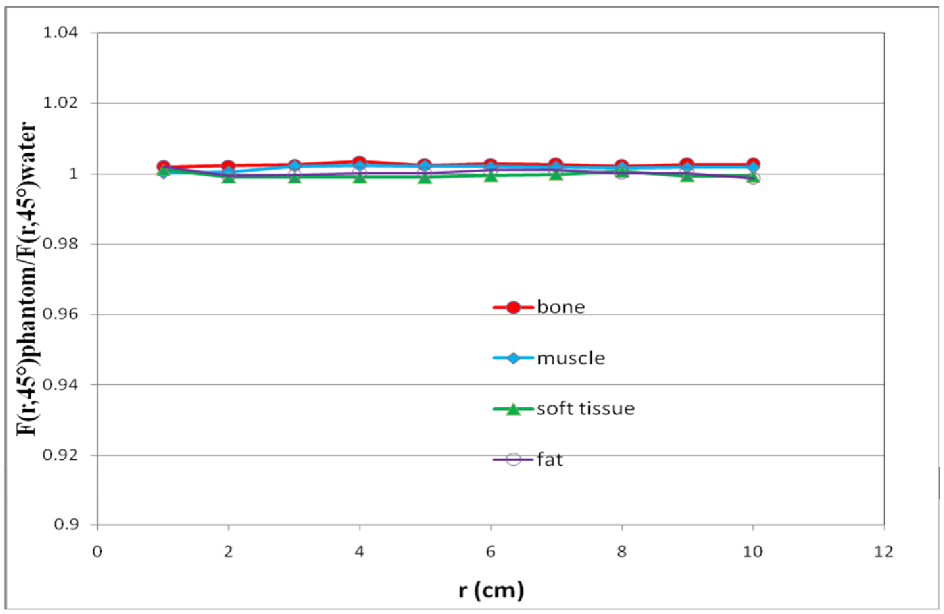

Figure 7. The ratio of the anisotropy function of Cs-137 in different phantoms to the anisotropy function of water angle=45°.

Figure 7 shows the ratio of anisotropy function of the tissues to the anisotropy function of water. As it is evident from the figure, the ratio of F(r,θ) is approximately equal to 1.

3.3. The effect of phantom material on dose distribution around ten active sources

As different configurations of active spherical sources and dummy spheres are used in the treatment of patients, the effect of phantom material was obtained for a standard combination of ten active sources and the values of dose rate on the transverse axis of the source (θ=90°) were compared for different phantoms. According to the results of the simulations, the dose rate on the transverse axis of the bone varies from 430.8 cGy/h at 1 cm to about 8.5 cGy/h at 9 cm, and these values vary from 446.9 cGy/h at 1 cm to 10.3 cGy/h at 9 cm.

Figure 8 shows the variation of doses rate in different phantoms from a 6 to 10 cm distance from the source.

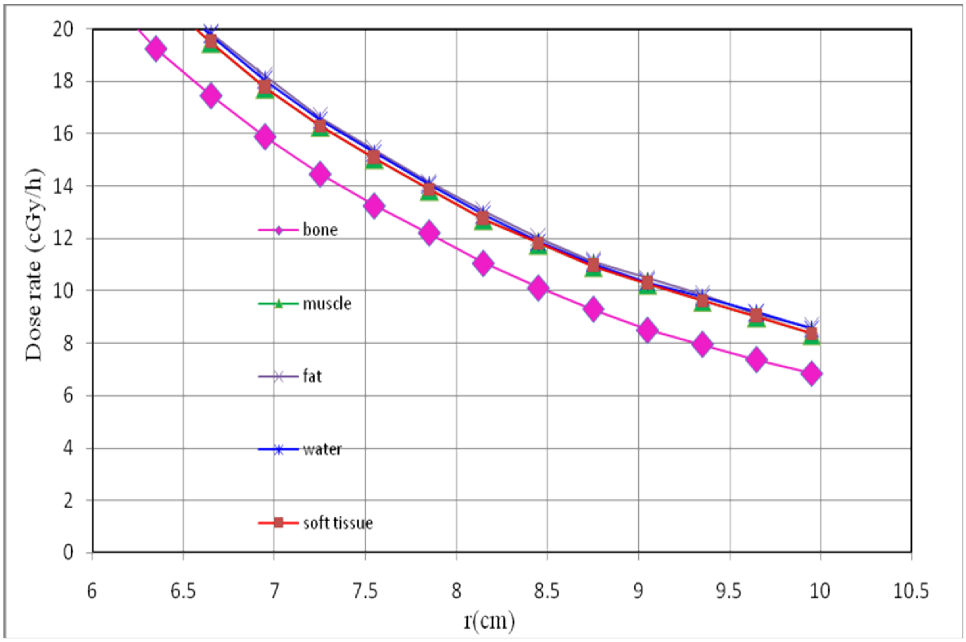

Figure 8. The variation of the dose rate in the transverse axis of a configuration of 10 active sources at different distances.

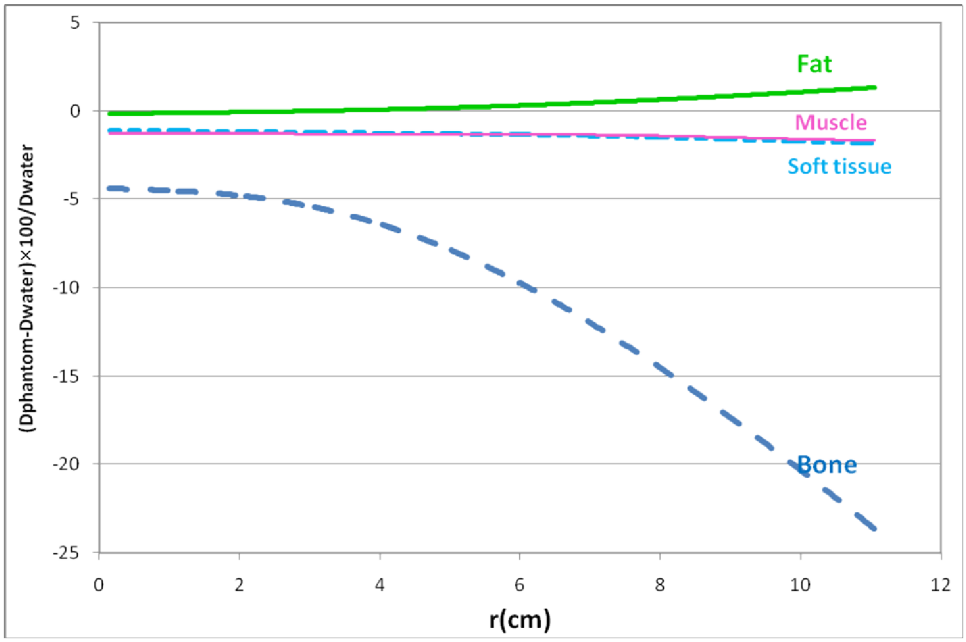

Figure 9. The percentage difference between the dose in different distances of different phantoms along the transverse axis (θ=90°) of a configuration of 10 active pellets, to the dose at the same distances in water phantom.

The maximum difference between the phantom doses and water doses is, again, for bone phantom. The percentage differences between the dose values on the transverse axis of different phantoms and water dose are shown in Figure 9.

4. Discussion and Conclusion

Comparisons of the isodose curves around the Cs-137 source inside the applicator show that considering the homogeneous water phantom instead of different tissues of the body would cause errors in dose calculations around the source. Comparison of the isodose curves of Figure 3 shows that the isodose curves inside

soft tissue, muscle, and fat are consistent with those inside the water phantom, and the maximum differences are observed for bone phantom. The main causes of these discrepancies are the different density, composition, effective atomic number, absorption, and attenuation coefficients of the two phantoms.

Comparison of the dose rate constant (Λ) in water with other tissues shows that the maximum difference between the value of the dose rate constant of the tissues with that of water is observed to be 4.52% for bone material, while such differences are 1.18%, 1.27%, and 0.18% for soft tissue, muscle, and fat, respectively. As can be seen in Table 1, the values of the dose rate constant obtained in this study are consistent with those obtained for Cs-137 by Melhus et al. using MCNP5 Monte Carlo code.

Comparison of the dose in different tissues with the water phantom (Figures 4 to 9), shows that the difference in doses in the two phantoms increases by increasing the distance from the source center such that, at a distance of 10 cm, the difference of the radial dose function of bone and water reaches 20% (Figure 4). Such an increase in the difference of the radial dose function can be explained by the fact that the average photon energy decreases by increasing the distance and this would cause an increase in the dependency of the dose rate on the atomic number of the phantom material. Results of this study are consistent with the results obtained by Melhus et al. for a linear Cs-137 source (without the applicator) in soft tissue and muscle, such that the radial dose function of these phantoms are equal to water up to a distance of 2 cm, and the difference then increases and at a distance of 10 cm, this difference reaches more than 20%.

It should be noted that the Cs-137 source simulated in this study is the Cs-137 model Selectron inside the applicator, while Melhus et al. performed the simulations using a linear brachytherapy source without the applicator.

To consider the real treatment, we have performed the simulations in inhomogeneous phantom composed of bone and water. Figure 5 shows the percentage difference in doses at different distances of inhomogeneous phantom (water/bone/water) with the dose in water. According to the results of the simulations, for the phantoms composed of a layer of water, a layer of bone, and a layer of water, the dose in the water layer before entering the bone increases slightly. This increase is due to the backscattered electrons form the water-bone boundary; after that, by entering the bone layer the dose decreases as the mass attenuation coefficient of water is less than water, and finally the dose at the third layer (water) is less than the dose at homogeneous water phantom, because of the shielding effect of the bone layer [1].

In addition, the radial dose function (g(r)), the dose in the transverse axis (θ=0°), and the dose at different angles are also dependent on the phantom material. This fact can be seen in Figure 6 for θ=45°. In this case, the highest percentage difference is for the doses at the points located on the axis θ=45° of bone and water, such that the difference between the dose of bone and water at r=5 cm and θ=45° is 0.96%.

According to the TG-43 protocol, the 2D anisotropy function of brachytherapy sources is the ratio of the dose at different distances at each angle to the dose at the same distance and 90° angle, by applying the ratios of geometry function.

As the dose differences at different angles (i.e. 45° and 90°) increase with increasing the distance, the ratio of the anisotropy function at 45°, (F(r, 45°)) and the anisotropy function at 90°, (F(r, 90°)) is constant with the distance (Figure 7). The values of F(r, θ) at different angles in different phantoms are also equal to F(r, θ) at water.

Table 1. The values of dose rate constant (Λ) for different tissues

Phantom		Soft tissue	Muscle	Fat	Bone	Water
Dose rate constant (Λ) cGyh-1U-1	This work	1.093±0.006	1.093±0.006	1.104±0.004	1.056±0.010	1.106±0.005
(Λphantom-Λwater)|*100/Λwater|	This work	1.18%	1.27%	0.18%	4.52%	0
(Λphantom/ Λwater) or D(r0,θ0)Phantom/D(r0,θ0)Water	This work	0.988%	0.987%	0.998	0.954	1
D(r0,θ0)Phantom/D(r0,θ0)Water	Melhus et al. [17]	0.989	0.991%	-----	-----	1

According to the results of this study, the dose rate constant and radial dose function of Cs-137 brachytherapy are dependent on the phantom material, but the anisotropy function is independent of the phantom material.

According to these results, considering the homogeneous water phantom would introduce the errors in dose calculations in treatment planning systems, especially in the presence of bone. Therefore, it is suggested that the results of the simulations and calculations of dosimetric parameters be corrected for the inhomogeneous phantoms to reduce the errors of dose calculations.

It is expected that the difference between the dosimetric parameters of low energy brachytherapy sources, i.e., Pd-103 and I-125, in different tissues compared with those of water be higher than the results of Cs-137. Therefore, it is suggested that similar studies be performed for other brachytherapy sources such as Pd-103, I-125, and Ir-192, and that the correction factors be obtained for correcting the dosimetry parameters in different phantoms.

Acknowledgment

The authors would like to thank the personnel of the Radiation Research Center of Shiraz University in performing this project.

References

1. Khan FM. The physics of radiation therapy .3th ed. Philadelphia: Lippincott Williams and Wilkins; 2003. p.560.
2. Nath R, Anderson LL, Luxton G, Weaver KA, Williamson JF, Meigooni AS. Dosimetry of interstitial brachytherapy sources: recommendations of the AAPM Radiation Therapy Committee Task Group No. 43. American Association of Physicists in Medicine. Med Phys. 1995; 22(2):209-34.
3. Markman J, Williamson JF, Dempsey JF, Low DA. On the validity of the superposition principle in dose calculations for intracavitary implants with shielded vaginal colpostats. Med Phys. 2001; 28(2):147-55.
4. Sina S, Faghihi R, Meigooni AS, Mehdizadeh S, Mosleh Shirazi MA, Zehtabian M. Impact of the vaginal applicator and dummy pellets on the dosimetry parameters of Cs-137 brachytherapy source. J Appl Clin Med Phys. 2011; 12(3):3480.
5. Rivard MJ, Venselaar JL, Beaulieu L. The evolution of brachytherapy treatment planning. Med Phys. 2009; 36(6):2136-53.
6. Sina S, Faghihi R, Meigooni AS, Mehdizadeh S, Zehtabian M, Mosleh-Shirazi MA. Simulation of the shielding effects of an applicator on the AAPM TG-43 parameters of Cs-137 Selectron LDR brachytherapy sources. Iran J Radiat Res. 2009; 7(3):135-40.
7. Pérez-Calatayud J, Granero D, Ballester F. Phantom size in brachytherapy source dosimetric studies. Med Phys. 2004; 31(7):2075-81.
8. Pérez-Calatayud J, Granero D, Ballester F, Lliso F. A Monte Carlo study of intersource effects in dome-type applicators loaded with LDR Cs-137 sources. Radiother Oncol. 2005;77(2):216-9.
9. Pérez-Calatayud J, Granero D, Ballester F, Puchades V, Casal E. Monte Carlo dosimetric characterization of the Cs-137 selectron/LDR source: evaluation of applicator attenuation and superposition approximation effects. Med Phys. 2004; 31(3):493-9.

10. Rivard MJ, Butler WM, DeWerd LA, Huq MS, Ibbott GS, Meigooni AS, et al. Supplement to the 2004 update of the AAPM Task Group No. 43 Report. Med Phys. 2007 Jun;34(6):2187-205.
11. Briemeister JF. MCNP - A General Monte Carlo N-Particle Transport Code. Version 4C Ed. Los Alamos New Mexico:Los Alamos National Laboratory 2001.
12. Rivard MJ, Coursey BM, DeWerd LA, Hanson WF, Huq MS, Ibbott GS, et al. Update of AAPM Task Group No. 43 Report: A revised AAPM protocol for brachytherapy dose calculations. Med Phys. 2004; 31(3):633-74.
13. International Commission on Radiation Units and Measurements (ICRU). Tissue Substitutes in Radiation Dosimetry and Measurements, ICRU Report 44. Bethesda, Maryland: ICRU Publications; 1989.
14. Fragoso M. Application of Monte Carlo Techniques for the Calculation of Accurate Brachytherapy Dose Distributions [PhD thesis]. The Institute of Cancer Research and The Royal Marsden NHS Trust: University of London; 2004.
15. Fragoso M, Love PA, Verhaegen F, Nalder C, Bidmead AM, Leach M, et al. The dose distribution of low dose rate Cs-137 in intracavitary brachytherapy: comparison of Monte Carlo simulation, treatment planning calculation and polymer gel measurement. Phys Med Biol. 2004; 49(24):5459-74.
16. Sina S, Faghihi R , Zehtabian M , Mehdizadeh S. Investigation of the Anisotropy Caused by a Cylinder Applicator on Dose Distribution around Cs-137 Brachytherapy Sources using the MCNP4C Code. Iran J Med Phys. 2011; 8(2):45:52.
17. Melhus CS ,Rivard MJ. Approaches to calculating AAPM TG-43 brachytherapy dosimetry parameters for 137Cs, 125I, 192Ir, 103Pd, and 169Yb sources. Med Phys. 2006; 33(6):1729-37.